A liquid-crystal model for friction

C.H. A. Cheng [*], **L. H. Kellogg** [†], **S. Shkoller** [*], **and D. L. Turcotte** [†]

[*]Department of Mathematics, University of California, Davis, CA 95616, and [†]Department of Geology, University of California, Davis, CA 95616

Contributed by D. L. Turcotte, November 19, 2007

Rate-and-state-friction is an empirical approach to the behavior of a frictional surface. We use a nematic liquid-crystal in a channel between two parallel planes to model frictional sliding. Nematic liquid-crystals model a wide variety of physical phenomena in systems that rapidly switch between states; they are well-studied and interesting examples of anisotropic non-Newtonian fluids, characterized by the orientational order of a director field $\vec{d}(\vec{x},t)$ interacting with the the velocity field $\vec{u}(\vec{x},t)$. To model frictional sliding, we introduce a *nonlinear* viscosity that changes as a function of the director field orientation; the specific choice of viscosity function determines the behavior of the system. In response to sliding of the top moving plane, the fluid undergoes a rapid increase in resistance followed by relaxation. Strain is localized within the channel. The director field plays a role analogous to the state variable in rate-and-state friction.

friction | faulting | rheology

Frictional rheologies have a wide range of applications in engineering and geophysics but are poorly understood (2). In this paper we present a nematic liquid-crystal model for friction in which the physical properties of the fluid varies with the orientation of the director field. We consider a fluid layer of prescribed thickness between two solid blocks. The blocks slide past each other at a prescribed slip velocity u_0. The objective is to determine the resulting shear stress which we take to be the frictional resistance. We take the fluid to be a liquid-crystal which introduces a relaxation process. A fluid-based model is directly applicable to wet friction, which occurs for example when a layer of oil is used to lubricate two sliding surfaces; however, a fluid model can also be justified for sliding friction. Dry friction between two sliding surfaces generates granulation, resulting in the development of a granular media between the surfaces. In the case of a geologic fault, this granular material is known as fault gauge and is widely recognized (9). It is standard practice to model a shear flow in a granular material as a fluid (7).

Nematic liquid-crystals are well-studied examples of anisotropic non-Newtonian fluids. A liquid-crystal is a phase of a material between the solid and liquid phases. The solid phase has strong intermolecular forces that keep the molecular position and orientation fixed, while in the liquid phase, the molecules neither occupy a specific average position nor do they remain in any particular orientation; the nematic liquid crystal phase does not have any positional order, but does possess a certain amount of orientational order. This phase is described by a velocity field, as well as a director field that describes locally the averaged direction or orientation of the constituent molecules (5).

A variety of friction laws have been proposed. Several empirical friction laws have been written to explain laboratory studies. These fall under the general class called rate-and-state friction (3,6,8). Probably the most widely accepted form of rate-and-state friction is the slowness law that can be written as

$$\mu = \mu_0 + a\ln\left(\frac{u}{u_0}\right) + b\ln\left(\frac{u_0\theta}{\mathcal{L}}\right), \qquad \frac{d\theta}{dt} = 1 - \frac{\theta u}{\mathcal{L}}, \quad [\mathbf{1}]$$

where u is the slip velocity, μ is the coefficient of friction, μ_0 is the reference coefficient of friction at the reference velocity u_0, θ is the state variable which can be considered to be a measure of healing and damage, $\mathcal{L}$ is a characteristic slip length associated with the healing, and a and b are parameters.

The characteristic behavior of these equations is illustrated by a step increase in the slip velocity from u_0 to u_1. The friction coefficient increases instantaneously to the value

$$\mu_i = \mu_0 + a\ln\left(\frac{u_1}{u_0}\right) \quad [\mathbf{2}]$$

A relaxation of the friction coefficient value then takes place to the final value given by

$$\mu = \mu_0 - (b-a)\ln\left(\frac{u_1}{u_0}\right) \quad [\mathbf{3}]$$

If $b > a$ the final coefficient of friction decreases with increasing velocity. This is velocity weakening and leads to the stick-slip behavior associated with faults.

Liquid-Crystal Model

Here, we use a liquid-crystal fluid, flowing in a horizontal channel between two parallel plates, to model frictional sliding (Fig. 1). Liquid crystals are extensively studied and have applications to a wide variety of engineered systems, including systems that rapidly switch between states(5). The liquid crystal is characterized by a directional field, $\vec{d}(y,t)$ where y is the vertical distance from the fixed lower plate and t is time.

The viscosity is given by $\nu = \alpha(\theta)\nu_1 + (1-\alpha(\theta))\nu_0$ where θ is the angle of the director field $\vec{d}$ with respect to the vertical. The minimum viscosity ν_0 occurs when $\vec{d}$ points in the horizontal direction, while the maximum viscosity ν_1 occurs when $\vec{d}$ is vertical. The choice of the function $\alpha(\theta)$ determines the type of friction that we simulate.

A third parameter γ denotes the relaxation coefficient of the director $\vec{d}$. When the velocity of the upper plate $\bar{u}$ is suddenly increased, the fluid undergoes a rapid increase in resistance, followed by a relaxation. The director $\vec{d}$ is deflected from the vertical, and strain is localized near the center of the channel. The director field $\vec{d}$ plays a role analogous to the state variable in rate-and-state friction. Reducing the relaxation coefficient γ of $\vec{d}$ produces a sharper increase in traction change as a function of velocity, but when γ is very small, numerical instability can enter the simulation. Reducing the minimum viscosity ν_0 to 0 produces stick-slip-like behavior, but restricts the choice of the function $\alpha(\theta)$; the choice of $\alpha(\theta)$, in turn, controls both the size of the traction jump associated with changes in velocity and the resulting relaxation back to the equilibrium state.

Conflict of interest footnote placeholder

The model is described by the following equations of motion. Conservation of momentum requires that

$$\vec{u}_t + (\vec{u}\cdot\nabla)\vec{u} = \mathrm{div}(\nu\nabla\vec{u}) - \frac{1}{\rho}\nabla p \quad \text{in } (0,T)\times\Omega\,, \qquad [4]$$

Where $\vec{u}$ is the velocity, ρ is density, ν is kinematic viscosity, and p is pressure, Ω denotes either a two- or three-dimensional smooth open set, and $[0,T]$ denotes the interval of time t on which we study the evolution of this system.

We assume that the fluid is incompressible, so that

$$\mathrm{div}\,\vec{u} = 0 \qquad \text{in } [0,T)\times\Omega\,, \qquad [5]$$

The viscosity in the fluid is determined by the orientation of the vector director field, $\vec{d}$. The director field behaves in a manner analogous to the velocity:

$$\vec{d}_t + \nabla\vec{d}\cdot\vec{u} - \nabla\vec{u}\cdot\vec{d} = \gamma\Delta\vec{d} \qquad \text{in } (0,T)\times\Omega\,, \qquad [6]$$

where γ is a relaxation parameter that plays a role analogous to the viscosity in Eq. [4]. Note that there is an interaction between the velocity field $\vec{u}$, which changes the orientation of the director field $\vec{d}$; the director field feeds back to the velocity field through its influence on viscosity.

The viscosity of the fluid ν depends on a function α which depends only on the angle θ between the director field and the fluid velocity. We choose a relationship between ν and α that is based on the behavior of liquid-crystals (2) but modified to yield a friction-like behavior.

$$\nu = \alpha(\theta)\nu_1 + (1-\alpha(\theta))\nu_0\,, \quad \text{in } (0,T)\times\Omega\,, \qquad [7]$$

where $\cos\theta = \|\vec{u}\times\vec{d}\|/(\|\vec{u}\|\|\vec{d}\|)$. The required initial and boundary conditions are taken to be

$$\vec{u} = \vec{u}_{BC} \qquad \text{on } [0,T)\times\partial\Omega\,, \qquad [8]$$

$$\vec{d} = \vec{d}_{BC} \qquad \text{on } [0,T)\times\partial\Omega\,, \qquad [9]$$

$$\vec{u} = \vec{u}_{\mathrm{ic}} \qquad \text{on } \{t=0\}\times\Omega\,, \qquad [10]$$

$$\vec{d} = \vec{d}_{\mathrm{ic}} \qquad \text{on } \{t=0\}\times\Omega\,, \qquad [11]$$

where subscript BC and ic denote specified boundary and initial conditions.

To use this model to characterize the behavior of a fault, we consider a two-dimensional infinite channel so that $\Omega = (-\infty,\infty)\times(0,L)$ with coordinates (x,y). The channel is filled with a fluid and we take the horizontal pressure gradient to be zero so that the flow is driven by the imposed velocity of the upper boundary of the channel $\vec{u}$.

We let $\vec{u}(x,y) = (u_1(x,y), u_2(x,y))$ and similarly $\vec{d}(x,y) = (d_1(x,y), d_2(x,y))$. Proceeding with the usual channel flow assumptions, we assume that the vertical component of the velocity field vanishes so that $u_2 = 0$, and that the horizontal component only depends on the vertical coordinate y. We set $u(y) := u_1(y)$. For the channel geometry we set $d_2 = 1$, and assume that the horizontal component d_1 only depends on the vertical coordinate so that we now take

$$d(y) := d_1(y) \qquad [12]$$

The model is illustrated in Fig. 1.

With these assumptions, and using the notation $u' = \frac{\partial u}{\partial y}$, the full system of equations simplifies as follows:

$$u_t = (\nu u')' \qquad \text{in } (0,T)\times(0,L) \qquad [13]$$

$$d_t = \gamma d'' + u' \qquad \text{in } (0,T)\times(0,L) \qquad [14]$$

$$\cos\theta = (1+d^2)^{-1/2} \qquad \text{in } (0,T)\times(0,L) \qquad [15]$$

$$\nu = \alpha(\theta)\nu_1 + (1-\alpha(\theta))\nu_0, \qquad \text{in } (0,T)\times(0,L) \qquad [16]$$

$$u(0,t) = 0,\ u(L,t) = \bar{u} \qquad t \geq 0 \qquad [17]$$

$$d(0,t) = d(L,t) = 0 \qquad t \geq 0 \qquad [18]$$

$$u(y,0) = \frac{\bar{u}(0)}{L}y \qquad 0 \leq y \leq L \qquad [19]$$

$$d(y,0) = 0 \qquad 0 \leq y \leq L \qquad [20]$$

where $\bar{u}(0)$ is the initial sliding velocity of the top plate.

In order to simplify our analysis it is appropriate to introduce non-dimensional variables. Our reference length is the channel width L, our reference velocity is the initial prescribed velocity of the upper boundary $\bar{u}(0)$; the reference viscosity is the viscosity at the boundaries ν_1 where $\theta = 0$, and the reference time is $L/\bar{u}(0)$. The derived non-dimensional parameters are the Reynolds number:

$$\mathbf{Re} = \frac{\bar{u}(0)L}{\nu_1}$$

which governs the viscous behavior, and the director number,

$$D = \frac{\nu_1}{\gamma}$$

The director number D is the ratio of the diffusion coefficient for vorticity, the kinematic viscosity ν_1, to the diffusion coefficient for the director field, γ. It is also the ratio of the relaxation time for the two processes. If $D >> 1$ the velocity field relaxes in a much shorter time than the director field. If $D << 1$, the director field relaxes in a much shorter time than the velocity field. Since D is the ratio of two relaxation times, it resembles, but is not equivalent to, either the Deborah number (8), which is the ratio of the relaxation time of a viscous material to the timescale for observation, or the Weissenberg number, the ratio of a relaxation time to a process time for a viscoelastic material.

Let $u \mapsto \bar{u}(0)u$; $\bar{u} \mapsto \bar{u}(0)\bar{u}$; $y \mapsto Ly$; $t \mapsto Lt/\bar{u}(0)$, $d \mapsto d_0 d$ and $\nu \mapsto \nu_1\nu$ be the changes of variables; then Eqs.

13 to **20** become

$$u_t = \frac{1}{\mathbf{Re}}(\nu u')' \qquad \text{in } (0,T)\times(0,1) \qquad [\mathbf{21}]$$

$$d_t = \frac{1}{D\mathbf{Re}}d'' + u' \qquad \text{in } (0,T)\times(0,1) \qquad [\mathbf{22}]$$

$$\cos\theta = (1+d^2)^{-1/2} \qquad \text{in } (0,T)\times(0,1) \qquad [\mathbf{23}]$$

$$\nu = \alpha(\theta)\nu_1 + (1-\alpha(\theta))\nu_0, \qquad \text{in } (0,T)\times(0,1) \qquad [\mathbf{24}]$$

$$u(0,t) = 0, u(1,t) = \bar{u} \qquad t \geq 0 \qquad [\mathbf{25}]$$

$$d(0,t) = d(1,t) = 0 \qquad t \geq 0 \qquad [\mathbf{26}]$$

$$u(y,0) = y \qquad 0 \leq y \leq 1 \qquad [\mathbf{27}]$$

$$d(y,0) = 0 \qquad 0 \leq y \leq 1 \qquad [\mathbf{28}]$$

We define a smooth transition function α from the minimum to maximum states of viscosity in Eq. **16**. We choose

$$\alpha(\theta) = \begin{cases} 1 & \text{if} \quad 0.9 \leq \cos\theta \leq 1 \\ \dfrac{e^{10\cos\theta}-1}{e^9-1} & \text{if} \quad 0 \leq \cos\theta \leq 0.9 \end{cases} \qquad [\mathbf{29}]$$

and this dependence is illustrated in Fig. 2. The model is now fully prescribed.

Simulations

Using numerical solutions to this highly nonlinear model, we will examine its behavior. We first give the results in the steady state. The shear stress (traction) τ is a constant across the channel. Using our non-dimensionalization we have $\tau \mapsto \nu_1\bar{u}(0)\tau/L$. We give the dependence of the non-dimensional traction τ and the maximum value of the horizontal component of the director field $d_{\max}$ on the Reynolds number in Fig. 3 for two values of the director number $D = 30$ and $D = 300$. The dependence on the Reynolds number is equivalent to a dependence on the velocity of the upper plate $\bar{u}$. It is seen that in both cases we have velocity strengthening for small **Re** (small $\bar{u}$) and velocity weakening for large **Re** (large $\bar{u}$). The velocity weakening behavior is similar to that of rate and state friction but without the singular behavior at $\bar{u} = 0$.

The maximum of the director d indicates the largest angle the director is deflected by the fluid. In both cases, it increases linearly initially, while starting to increase more rapidly when it is bigger than 0.5. Note that when $d > 0.5$, $\cos\theta = (1+d^2)^{-1/2}$ is smaller than 0.9, in which case α starts to drop dramatically. When this occurs, τ, the traction at the top, decreases accordingly.

The laboratory experiments that have been used to derive the rate-and-state friction laws utilize a sudden increase of the sliding velocity from $\bar{u}(0)$ to $\bar{u}(0) + \delta u$ and then a sudden decrease back to $\bar{u}(0)$ (3,4,6,8). We next study the transient response of the liquid-crystal layer to a rapid change in the top-plate sliding velocity $\bar{u}$. In the following two simulations, a tanh(tan)-type of transition is considered: the top plate sliding velocity is defined as

$$\bar{u} = \begin{cases} 1 & \text{if} \quad t \in [0, 14.9]\,, \\ \mathbf{u} + \dfrac{\delta u}{2}\tanh[\tan(5(t-15)\pi)] & \text{if} \quad t \in [14.9, 15.1]\,, \\ 1 + \delta u & \text{if} \quad t \in [15.1, 19.9]\,, \\ \mathbf{u} - \dfrac{\delta u}{2}\tanh[\tan(5(t-20)\pi)] & \text{if} \quad t \in [19.9, 20.1]\,, \\ 1 & \text{if} \quad t \in [20.1, 25]\,. \end{cases} \qquad [\mathbf{30}]$$

where $\mathbf{u} = 1 + \delta u/2$. The change of the top plate sliding velocity is shown in Figure 4. This dependence is a close approximation to a step increase followed by a step decrease in the upper plate velocity.

We now give numerical solutions for two examples:
Case 1: Re $= 0.04129$, $D = 300$ and $\delta u = 0.0145$.
Case 2: Re $= 0.02443$, $D = 30$ and $\delta u = 0.0914$.

The steady state behavior of these cases is illustrated in Fig. 3. It is seen that Case 1 is in a velocity weakening region and Case 2 is in a velocity strengthening region. The final steady-state structure of Case 1 is illustrated in Fig. 5 for $t = 25$. The profiles of velocity u, director d, viscosity ν, and director angle θ are given. It is seen that the fluid shear is strongly concentrated near the center of the channel where d is maximum and the viscosity ν and angle θ are minima.

The dependence of the non-dimensional traction force τ on time t is given in Fig. 6 for the two cases. The dependence of the maximum horizontal value of the traction field d on time t is given in Fig. 7 for the two cases. For both cases there is a rapid increase in the traction force τ when the velocity is changed. The director field has not relaxed so that the viscosity is nearly constant during the velocity transient. In both cases there is a transient increase of the maximum value of the horizontal component of the director field. This leads to a decrease in θ and a decrease in the viscosity ν near the center of the channel. In Case 1, the decrease in the traction force is greater than the initial increase so that the steady state traction force at the higher velocity $\bar{u} = u_2$ is less than the initial value at $\bar{u} = 1$. This corresponds to the velocity weakening behavior for this case as shown in Fig. 3a. There is also a decrease in the traction force during the transient in Case 2. But the decrease is less than the initial increase so that the steady state traction force at the higher velocity $\bar{u} = u_2$ is greater than the initial value at $\bar{u} = 1$. This corresponds to the velocity strengthening behavior given for this case in Fig. 3b. A mirror image behavior is seen when the velocity is returned to its initial value $\bar{u} = 1$ in the two cases.

Discussion

In this paper we have introduced a liquid-crystal model for friction. The objective is to compare the behavior of this model with the empirical rate-and-state slowness law illustrated in Eqs. **1** and **3**. The steady-state behavior of the liquid-crystal model is illustrated in Fig. 3. At low Reynolds numbers (low velocities) the traction increases with an increase in Reynolds number (velocity). This is velocity strengthening and solutions are stable. At high Reynolds number (high velocities) the traction decreases with an increase in Reynolds number (velocity). This is velocity weakening and solutions are unstable, leading to stick-slip behavior.

The transient behavior of the liquid-crystal model is illustrated with two cases. Case 1 is the unstable velocity-weakening region and Case 2 is the stable velocity-strengthening region. The velocity-weakening Case 1 is very similar to the transient behavior of rate and state friction when $a > b$. The velocity-strengthening Case 2 is very similar to rate and state friction when $b > a$.

The velocity-weakening friction is directly responsible for the stick-slip behavior of faults and the occurrence of earthquakes. The empirical rate-and-state friction laws based on laboratory experiments reproduce the velocity weakening friction but the basic physics of this behavior is poorly understood. The physics of the velocity weakening in our liquid-crystal model is clear. It is a direct result of the coupling between the director field and the velocity field through the viscosity. An increase in fluid shear results in an alignment of the director field with the flow and a reduction in the viscosity. This reduction leads to the reduction of the traction and velocity weakening.

The alignment of the director field is a transient processes obeying the diffusion equation as can be seen from Eq. **6**. The weakening associated with rate-and-state friction has a similar relaxation from velocity strengthening at short times to velocity weakening at long times.

Friction is attributed to the roughness of surfaces and/or the interactions of the granular material between the surfaces. The interacting surfaces are generally referred to as asperities. We believe that it is appropriate to associate the reorientation of the director field to the horizontal direction at high velocities with the weakening of asperity contacts in faults at higher slip velocities. The validity of this association remains to be explored in detail.

This work was supported by NSF EAR 0327799

1. Blau PJ (1996) *Friction Science and Technology*, Dekker, New York.
2. Coutand D, Shkoller S (2001) *C R Acad Sci Paris Ser I Math* 333: 919–924.
3. Dieterich JH (1979) *J Geophys Res* 84: 2161–2168.
4. Dieterich JH, Kilgore BD (1994) *Pure and Applied Geophysics* 143: 283–302.
5. De Gennes PG, Prost J *The Physics of Liquid Crystals, 2nd Ed.*; Clarendon Press: Oxford, (1993).
6. Marone C (1998) *Ann Rev Earth Planet Sci* 26:643–696.
7. Nedderman RM (1992) *Statics and Kinematics of Granular Flows*, Cambridge University Press, Cambridge.
8. Reiner M (1964) *Physics Today* 17:62
9. Ruina AL (1983) *J Geophys Res* 88:359–370
10. Schulz CH (2002) *The Mechanics of Earthquakes and Faulting*, Cambridge University Press, Cambridge.

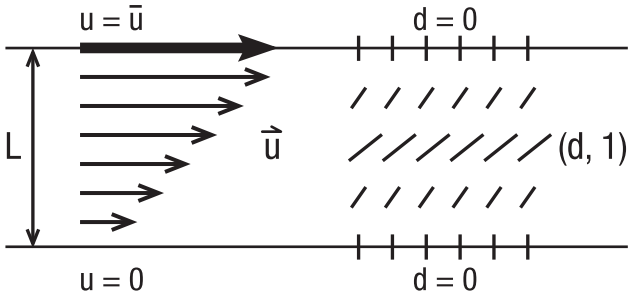

Fig. 1. Illustration of our fault model, a horizontal channel of thickness L filled with a liquid-crystal. The horizontal velocity u increases from $u = 0$ at the base to $u = \bar{u}$ at the top. The director field has a constant vertical component; the horizontal component is zero at the boundaries and increases to a maximum at the center.

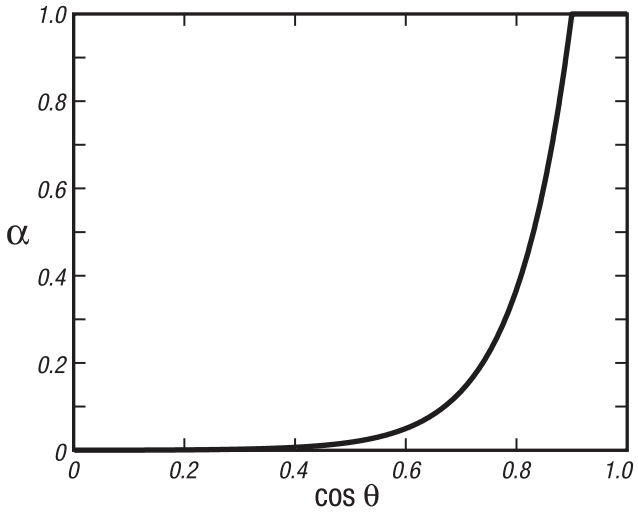

Fig. 2. Dependence of the transition function α for the viscosity as defined in Eq. $(\mathbf{16})$ on the angle of the director field θ

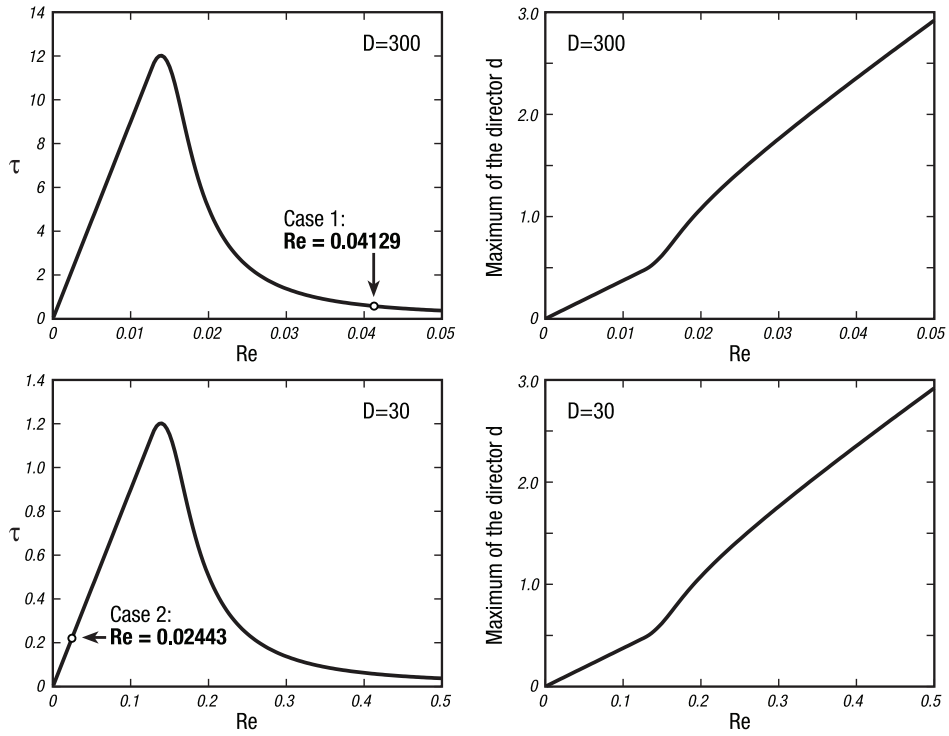

Fig. 3. Steady-state dependence of the non-dimensional traction τ and the maximum horizontal value of the traction field d on the Reynolds number $\mathbf{Re}$. Two values of the director number are considered: $D = 300$ and $D = 30$. Also shown are the Reynolds numbers of the two transient solutions that we present.

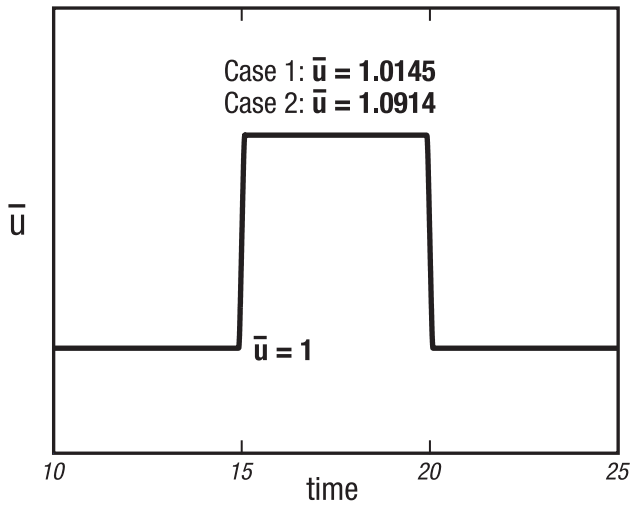

Fig. 4. Dependence of the non-dimensional top plate sliding velocity $\bar{u}$ on the non-dimensional time t for our transient simulations.

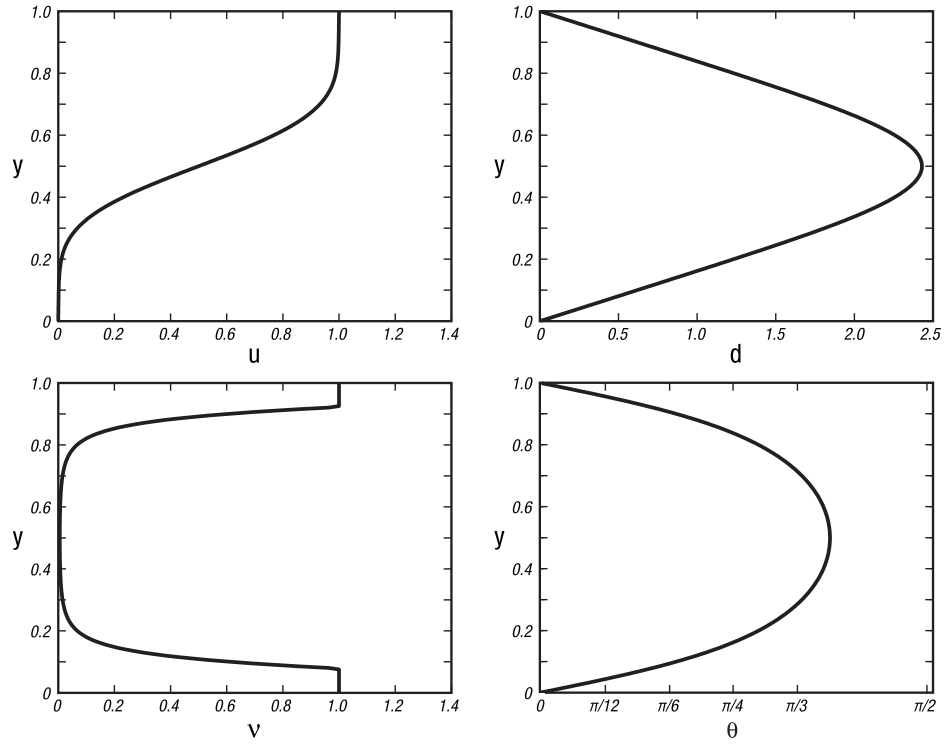

Fig. 5. Profiles of velocity u, director field d, viscosity ν, and director angle θ across the channel for Case 1 at time $t = 25$

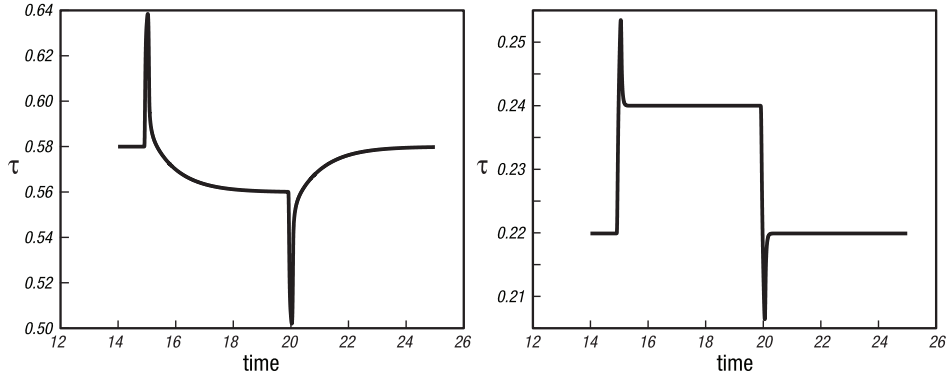

Fig. 6. Dependence of the non-dimensional traction force τ on time t for Case 1 (left) and Case 2 (right)

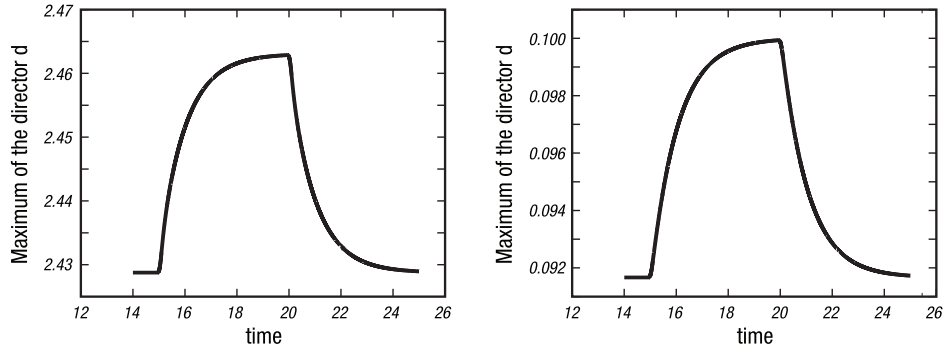

Fig. 7. Dependence of the maximum horizontal value of the director field d on time t for Case 1 (left) and Case 2 (right).